



Acceleration Effect of CuCN in Ag Electroplating for Ultralarge-Scale Interconnects

Sung Ki Cho,^a Jong Kyun Lee,^a Soo-Kil Kim,^{b,*} and Jae Jeong Kim^{a,*z}

^aResearch Center for Energy Conversion and Storage, School of Chemical and Biological Engineering, Seoul National University, Kwanak-gu, Seoul 151-742, Korea

^bCenter for Fuel Cell Research, Korea Institute of Science and Technology, Sungbuk-gu, Seoul 136-791, Korea

The addition of CuCN accelerated the deposition rate in cyanide-based Ag electroplating. The catalytic effect came from the high-order complexation of Cu with the free CN⁻ ions in electrolyte. It changed the equilibrium state of the electrolyte, presented as an increase in the amount of Ag(CN)₂⁻ compared to Ag(CN)₃²⁻. Because Ag(CN)₂⁻ could be reduced more easily, Ag electroplating was accelerated. Fourier transform infrared analysis showed the equilibrium change with the increase in Ag(CN)₂⁻ peak according to the CuCN addition. For superfilling, it is necessary to localize the complexation on the Cu surface.

© 2007 The Electrochemical Society. [DOI: 10.1149/1.2769103] All rights reserved.

Manuscript submitted May 17, 2007; revised manuscript received June 21, 2007. Available electronically August 3, 2007.

While Cu has been introduced successfully in microprocessors by damascene electroplating, Ag has a high potential for a next-generation interconnect material in ultralarge-scale interconnects (ULSI) because it has the lowest resistivity¹ and superior resistance in electromigration.²⁻⁷

Defect-free superfilling is essential for reliable metal interconnects in damascene electroplating and it is attained by the addition of a catalytic accelerator in the electrolyte. In Cu electroplating, accelerators on the Cu surface are accumulated at the trench-inside due to the reduction in the surface area at the concave of trench with the deposition. Locally crowded accelerator in the trench enhances the deposition rate and makes the superfilling.⁸⁻¹⁰ Some organic accelerators, for example, 3-mercapto-1-propane-sulfonic acid (MPSA),^{8,11-13} bis(3-sulfopropyl) disulfide, disodium salt (SPS),^{9,10,12,14,15} and 3-*N,N*-dimethylaminodithiocarbamoyl-1-propanesulfonic acid (DPS)¹⁶ are known as superfilling-capable accelerators. In Ag electroplating, there has been little research about accelerators. Our previous research showed successful Ag superfilling with benzotriazole (BTA) as an accelerator and thiourea as a suppressor in cyanide-based Ag electroplating.⁴ Baker et al.^{6,7} investigated the electrochemical characteristics and filling properties of SeCN⁻ as a single catalytic additive in cyanide-based Ag electroplating. Nevertheless, it is difficult to develop the various accelerators or to understand the reaction mechanism of the accelerator because the electroplating system of cyanide-based electrolyte is complex.

In this study, CuCN was developed as an accelerator in cyanide-based Ag electroplating. Its acceleration effect and the reaction mechanism were investigated through electrochemical and spectroscopic analyses.

Experimental

Substrates used herein were planar Si wafers with the structure of Ag {physical vapor deposition (PVD), 100 nm}/TiN {chemical vapor deposition (CVD), 10 nm}/Ti (PVD, 15 nm)/Si(100).

Ag electroplating was carried out with the cyanide-base electrolyte consisting of potassium Ag(I) cyanide [KAg(CN)₂, 0.92 M] and potassium cyanide (KCN, 1.1 M). 500 mL of electrolyte was prepared for the plating. CuCN was added in the electrolyte with various concentrations in the range of 0–200 mM. As CuCN was added, the plating was performed within 10 min. The working electrode of 1 cm² area was the Ag seeded substrate. An Ag wire (99.999%) and saturated calomel electrode (SCE) were used as a counter and a reference electrode, respectively. The deposition was conducted under the potentiostatic condition of –800 mV (vs SCE)

using PAR 263A potentiostat (EG&G Princeton Applied Research Corporation). The deposition was carried out for 60 s without agitation. After the deposition, the substrates were rinsed with deionized water and dried with N₂ gas blowing.

The acceleration effect of CuCN was observed through the monitoring of deposition thickness and electrochemical linear sweep voltammetry (LSV) according to the CuCN addition. The deposition thickness was measured with field-emission-scanning electron microscope (FESEM, JSM-6330F, JEOL). The LSV analyses were performed on a round Ag electrode with an area of 0.0314 cm² in the stagnant electrolyte condition. In each LSV analysis, the potential was swept in the range of –0.65 to –1.50 V (vs SCE) with a scan rate of 10 mV/s. Fourier transform infrared (FTIR) spectrometer analyses (Spectrum RX1, Perkin-Elmer) were also carried out on the electrolyte of Ag electroplating in order to observe the change in the electrolyte with CuCN addition. The peak positions of the Cu and Ag cyanide complexes are listed in Table I. The depth profile of the Ag film electroplated in the presence of CuCN was analyzed with Auger electron spectroscopy (AES, model 660, Perkin-Elmer).

Results and Discussion

Figure 1 shows the cross-sectional FESEM images of Ag films electroplated for 60 s at –800 mV (vs SCE) with the addition of CuCN (Fig. 1a-c) and the deposition rate according to the concentration of CuCN (Fig. 1d). When 186 mM of CuCN was added to the electrolyte (Fig. 1c), the film thickness increased by about 60% compared to the film deposited without CuCN (Fig. 1a). The deposition rate increased with the concentration of CuCN (Fig. 1d). The AES depth profile of Ag film electroplated with CuCN showed no Cu atoms in the film, which meant that the increase in the deposition rate was not originated from the codeposition of CuCN and it acted as an additive (Fig. 2). The acceleration effect of CuCN in deposition was also shown in the electrochemical LSV analysis (Fig. 3).

Table I. Infrared absorption frequencies (in the region 2000–2200 cm⁻¹) for various Cu and Ag cyanide complexes (Ref. 17).

Species	State	Wavenumber (cm ⁻¹)
Ag(CN) ₂ ⁻	Aqueous	2135 ± 1
Ag(CN) ₃ ²⁻	Aqueous	2105 ± 1
Ag(CN) ₄ ⁻	Aqueous	2092 ± 1
Cu(CN) ₂ ⁻	Aqueous	2125 ± 3
Cu(CN) ₃ ²⁻	Aqueous	2094 ± 1
Cu(CN) ₄ ⁻	Aqueous	2076 ± 1
CN ⁻	Aqueous	2080 ± 2
CuCN	Solid	2172 ± 1
AgCN	Solid	2164 ± 1

* Electrochemical Society Active Member.

^z E-mail: jkimm@snu.ac.kr

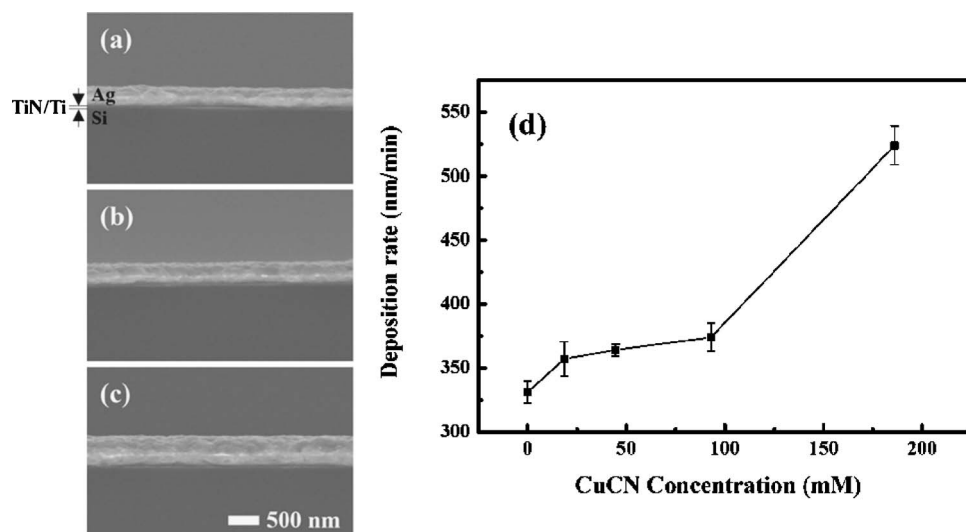
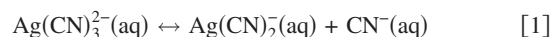


Figure 1. Cross-sectional FESEM images of Ag electrodeposited under the potentiostatic condition of -800 mV (vs SCE) for 60 s (a) without CuCN, (b) with 44.6 mM of CuCN, and (c) with 186.0 mM of CuCN. (d) Ag deposition rate according to the CuCN concentration evaluated by measuring the electroplated Ag film thickness.

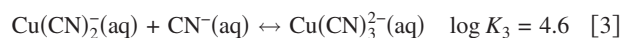
Although the current curve of 44.6 mM was similar to that of 18.6 mM, the current increased gradually as CuCN was added to the electrolyte in the potential range up to -1.0 V. However, over the potential of -1.0 V, the LSV curves crossed due to hydrogen

evolution.¹⁸ Still, it was obvious that the addition of CuCN led to the increase in current at -0.8 V, at which all depositions in this study were performed.

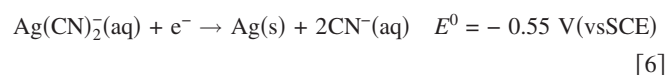
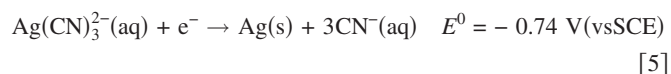
In cyanide-based Ag electroplating, various Ag complexes such as $\text{Ag}(\text{CN})_2^-$ and $\text{Ag}(\text{CN})_3^{2-}$ exist in the electrolyte. The predominant species involved in the charge-transfer reaction depends on CN^- concentration with the following equilibrium^{19,20}



According to Eq. 1, as CN^- concentration decreases, the main species in the electrolyte changes from $\text{Ag}(\text{CN})_3^{2-}$ to $\text{Ag}(\text{CN})_2^-$. The addition of CuCN might affect the CN^- concentration through the additional high-order complexation of Cu with the CN^- ions, resulting in the change of the equilibrium, the main deposition species, and the deposition mechanism in consequence. The complexation of Cu in a cyanide system is known to have a high stability constant (β) and high equilibrium constant (K), indicating preferential high-order complexation in the electrolyte^{19,21,22}



β_2 is a stability constant of $\text{Cu}(\text{CN})_2^-$. As CuCN was dissociated in the electrolyte, the Cu^+ ion formed the cyanide complexes by consuming free CN^- in the solution, so that the amount of $\text{Ag}(\text{CN})_2^-$ complexes increased and the amount of $\text{Ag}(\text{CN})_3^{2-}$ complexes decreased due to the lack of CN^- ion according to the equilibrium condition of Eq. 1. It changed in the current generated under the potentiostatic condition because the redox equilibrium potentials (E) of $\text{Ag}(\text{CN})_2^-$ and $\text{Ag}(\text{CN})_3^{2-}$ differed as follows²³



Sufficient $\text{Ag}(\text{CN})_2^-$ in the solution increased the current density at the constant electrode potential because a lower equilibrium potential of $\text{Ag}(\text{CN})_2^-$ resulted in a higher overpotential in the reduction for electroplating. Namely, the change in the equilibrium state of the electrolyte by adding CuCN produced the acceleration effect

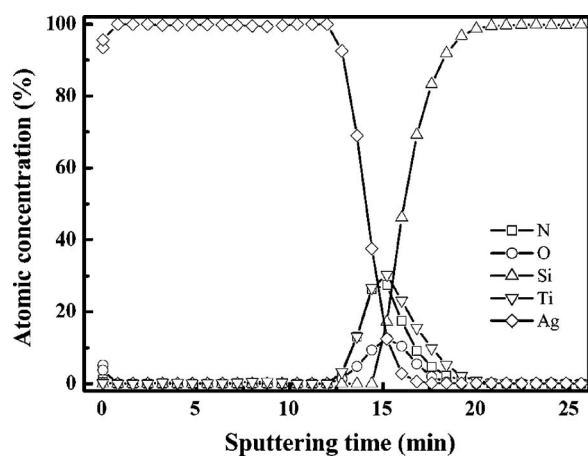


Figure 2. AES depth profile of Ag film deposited with 93.0 mM of CuCN.

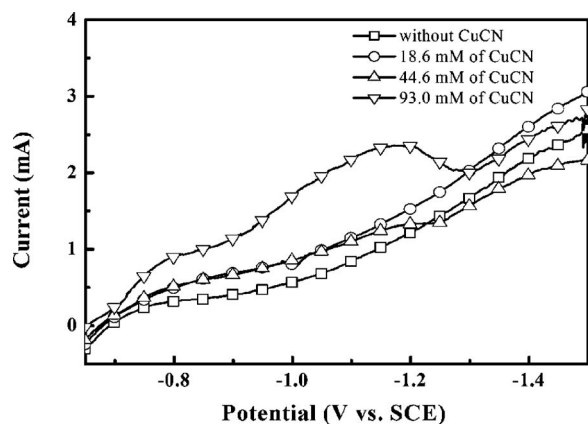


Figure 3. LSV with the addition of CuCN on Ag electrode. The potential was swept with the scan rate of 10 mV/s in the range of -0.65 to -1.50 V (vs SCE).

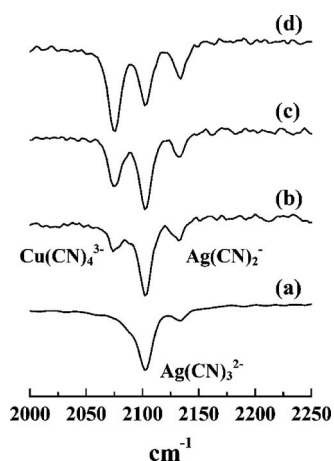


Figure 4. FTIR spectrometer analyses on the cyanide-based electrolyte contained (a) no CuCN, (b) 18.6 mM of CuCN, (c) 44.6 mM of CuCN, and (d) 93.0 mM of CuCN. The wavenumbers of $\text{Cu}(\text{CN})_4^{3-}$, $\text{Ag}(\text{CN})_3^{2-}$, and $\text{Ag}(\text{CN})_2^-$ were 2076, 2105, and 2135 cm^{-1} , respectively.

in Ag electroplating. Because the deposition rate depends on the change of the equilibrium, the acceleration would have increased nonlinearly with the concentration of CuCN as shown in Fig. 1d and LSV data.

FTIR analyses were conducted in order to observe the change in the equilibrium and the complexation of Cu in the electrolyte (Fig. 4). Various Ag and Cu cyanide complexes were detected from the analyses, as shown in the figure. When CuCN was not added in the electrolyte, a strong $\text{Ag}(\text{CN})_3^{2-}$ peak (2105 cm^{-1}) was observed, though the $\text{Ag}(\text{CN})_2^-$ peak (2135 cm^{-1}) was weak. As CuCN was added in the electrolyte, the intensity of the $\text{Ag}(\text{CN})_2^-$ peak increased. This meant that the addition of CuCN changed the equilibrium state of the solution and increased the amount of $\text{Ag}(\text{CN})_2^-$ in the electrolyte. This observation was well-matched with the explanation for the change in electrolyte condition due to CuCN. The other peak that increased with CuCN was related to $\text{Cu}(\text{CN})_4^{3-}$ (2076 cm^{-1}). It came from the complexation of Cu^+ in the electrolyte, but the peaks related to $\text{Cu}(\text{CN})_2^-$ (2125 cm^{-1}) and $\text{Cu}(\text{CN})_3^{2-}$ were very weak or not observed in analysis, which meant that Cu was fully complexed with CN^- in the electrolyte due to its high stability constant.

Actually, the change in the reaction rate and the equilibrium state in the electrolyte can be modulated by KCN, which is added to stabilize the complex and improve the conductivity of the bath. In particular, KCN is dissolved to generate the free CN^- ion. Because the equilibrium state and predominant species depend on the CN^- concentration, the addition of KCN affects the equilibrium state of the electrolyte. Accordingly, $(\text{Ag})/(\text{CN})$, that is, the ratio of the mole concentration of Ag added in the form of $\text{KAg}(\text{CN})_2$ which was maintained as constant in this study to the total amount of CN^- added with $\text{KAg}(\text{CN})_2$ and KCN, could represent the equilibrium state of the electrolyte. A higher $(\text{Ag})/(\text{CN})$ value means a relatively low amount of CN^- , so a high amount of $\text{Ag}(\text{CN})_2^-$ could be expected in the solution. The equilibrium changes with $(\text{Ag})/(\text{CN})$ values were observed with FTIR and electrochemical analyses, as shown in Fig. 5. Figure 5a shows FTIR analyses on the electrolytes with various $(\text{Ag})/(\text{CN})$ values. At the high value of $(\text{Ag})/(\text{CN})$, the peak of $\text{Ag}(\text{CN})_2^-$ becomes clear. Except for the absence of the Cu complex peak, the FTIR results were similar to those of the CuCN additions (Fig. 4). In other words, the change in the electrolyte condition with the CuCN addition was equal to the change in the equilibrium state with CN^- concentration. Figure 5b shows the variation of the deposition rate with the $(\text{Ag})/(\text{CN})$ value. The deposition rate

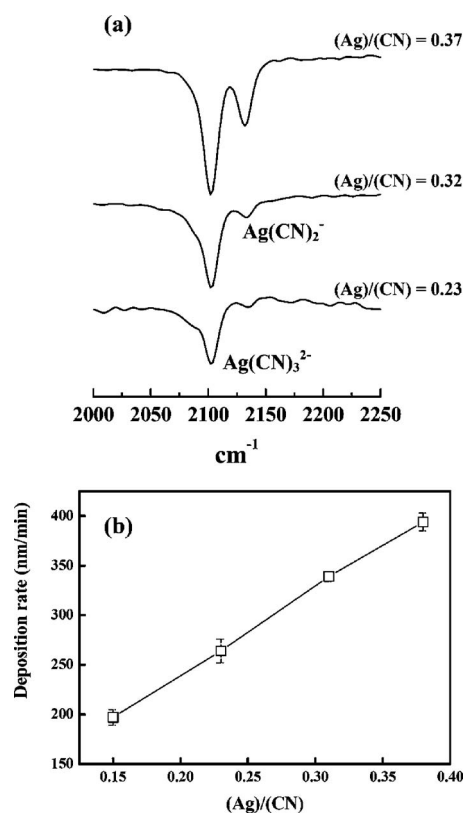


Figure 5. (a) FTIR spectrometer analyses on the cyanide-based electrolyte with various $(\text{Ag})/(\text{CN})$ values [$(\text{Ag})/(\text{CN}) = 0.23, 0.32,$ and 0.37] and (b) the deposition rate according to $(\text{Ag})/(\text{CN})$. $(\text{Ag})/(\text{CN})$ value is the total mole concentration of Ag added with $\text{KAg}(\text{CN})_2$ over the total amount of CN^- added with $\text{KAg}(\text{CN})_2$ and KCN.

increased with the $(\text{Ag})/(\text{CN})$ value because many $\text{Ag}(\text{CN})_2^-$ complexes, which could be reduced more easily compared to $\text{Ag}(\text{CN})_3^{2-}$, were generated. This evidence makes it clear that the equilibrium change by CuCN can vary the deposition rate.

The addition of CuCN consumed the free CN^- in the electrolyte due to its complexation with CN^- , leading to a change in the equilibrium state of the electrolyte and $\text{Ag}(\text{CN})_2^-$ dominated over $\text{Ag}(\text{CN})_3^{2-}$ in the cyanide-poor electrolyte state. When 93.0 mM of CuCN was added to the base electrolyte [0.92 M $\text{KAg}(\text{CN})_2$, 1.1 M KCN], 279.0 mM of free CN^- was consumed, assuming a full complexation as $\text{Cu}(\text{CN})_4^{3-}$. As a result, the $(\text{Ag})/(\text{CN})$ value in the electrolyte changed from 0.313 to 0.346. The change was related to the approximate deposition rate of 370 nm/min, described in Fig. 5b, and it was similar to the real deposition rate of 374 ± 11 nm/min generated with 93.0 mM of CuCN, as shown in Fig. 1d. This simple calculation can support the above-mentioned explanation of the phenomena of the catalytic effect of CuCN.

Until now, it was electrochemically and spectroscopically observed that the acceleration effect of CuCN (Cu ion to be exact) came from high-order complexation of Cu with free cyanide. However, it might not generate the local variation of the deposition rate and subsequent superfilling, because the complexation is related not to the surface but to bulk electrolyte. But it is possible to achieve superfilling if the complexation is bound on the surface. For example, Cu seed can be used as a complexing source. Baker et al.⁶ reported the dissolution of Cu seed in cyanide bath. Dissolved Cu ions can form high-order Cu cyanide complex as does CuCN. The Cu ions concentrated at trench-inside consume cyanide ions, enhance the local deposition rate, and finally make superfilling. This will be evaluated in succeeding research.

Conclusions

When CuCN was added in cyanide-based Ag electroplating, the deposition rate increased without incorporation of Cu. In the FTIR analyses, it was observed that CuCN changed the equilibrium state by consuming the free CN^- due to the formation of the Cu cyanide complex, $\text{Cu}(\text{CN})_4^{3-}$, in the electrolyte. A similar change in the equilibrium state, accomplished by varying the compositions of the electrolyte, showed a change in the deposition rate in electroplating. It was concluded that CuCN changed the equilibrium state and species that participated in the reduction, so that it varied the deposition rate.

Acknowledgments

This work was supported by the Korea Science and Engineering Foundation through the Research Center for Energy Conversion and Storage (RCECS), Dongbu HiTeK, and also by the Institute of Chemical Processes (ICP).

Seoul National University assisted in meeting the publication costs of this article.

References

1. R. Manepalli, F. Stepniak, S. A. Bidstorp-Allen, and P. A. Kohl, *IEEE Trans. Adv. Packag.*, **22**, 4 (1999).
2. M. Hauder, J. Gstöttner, W. Hansch, and D. Schmitt-Landsiedel, *Appl. Phys. Lett.*, **78**, 838 (2001).
3. T. L. Alford, Y. Zeng, P. Nguyen, L. Chen, and J. W. Mayer, *Microelectron. Eng.*, **55**, 389 (2001).
4. E. J. Ahn and J. J. Kim, *Electrochem. Solid-State Lett.*, **7**, C118 (2004).
5. T. P. Moffat, B. Baker, D. Wheeler, J. E. Bonevich, M. Edelstein, D. R. Kelley, L. Gan, G. R. Stafford, P. J. Chen, W. F. Egelhoff, and D. Josell, *J. Electrochem. Soc.*, **149**, C423 (2002).
6. B. C. Baker, C. Witt, D. Wheeler, D. Josell, and T. P. Moffat, *Electrochem. Solid-State Lett.*, **6**, C67 (2003).
7. B. C. Baker, M. Freeman, B. Melnick, D. Wheeler, D. Josell, and T. P. Moffat, *J. Electrochem. Soc.*, **150**, C61 (2003).
8. D. Josell, D. Wheeler, W. H. Huber, and T. P. Moffat, *Phys. Rev. Lett.*, **87**, 016102 (2001).
9. J. Reid, *J. Appl. Phys.*, **40**, 2650 (2001).
10. A. C. West, S. Mayer, and J. Reid, *Electrochem. Solid-State Lett.*, **4**, C50 (2001).
11. J. J. Kim, S.-K. Kim, and Y. S. Kim, *J. Electroanal. Chem.*, **542**, 61 (2003).
12. S.-K. Kim and J. J. Kim, *Electrochem. Solid-State Lett.*, **7**, C98 (2004).
13. T. P. Moffat, J. E. Bonevich, W. H. Huber, A. Stanishevsky, D. R. Kelly, G. R. Stafford, and D. Josell, *J. Electrochem. Soc.*, **147**, 4524 (2000).
14. S.-K. Kim, S. K. Cho, J. J. Kim, and Y.-S. Lee, *Electrochem. Solid-State Lett.*, **8**, C19 (2005).
15. T. P. Moffat, D. Wheeler, and D. Josell, *J. Electrochem. Soc.*, **151**, C262 (2004).
16. S. K. Cho, S.-K. Kim, and J. J. Kim, *J. Electrochem. Soc.*, **152**, C330 (2005).
17. R. A. Penneman and L. H. Jones, *J. Chem. Phys.*, **24**, 293 (1956).
18. H. C. Koo, E. J. Ahn, and J. J. Kim, *J. Electrochem. Soc.*, Submitted.
19. A. Gherrou and H. Kerdjoudj, *Desalination*, **151**, 87 (2002).
20. G. Baltrūnas, *Electrochim. Acta*, **48**, 3659 (2003).
21. J. Lu, D. B. Dreisinger, and W. C. Cooper, *Hydrometallurgy*, **66**, 23 (2003).
22. F. A. Lemos, L. G. S. Sobral, and A. J. B. Dutra, *Minerals Eng.*, **19**, 388 (2006).
23. A. J. Bard, R. Parsons, and J. Jordan, in *Standard Potentials in Aqueous Solution*, p. 305, IUPAC, New York (1985).